Supplementary Information

Boosting Photocatalytic Simultaneous Hydrogen Evolution and Plastic Reforming via Surface Hydroxylation over $NiMoO_4$/CdS Heterojunction: Interfacial Microenvironment and Electronic Structure Regulation

Zixu Hu, Wenjun Jiang, Yuxin Zhang, Ao Xu, Yangjie Wu, Liang Zhou, Juying Lei*, Jinlong Zhang**

Contents

1. Supplementary experiment

Characterization

X-ray diffraction (XRD) patterns were collected for all samples within a 5-80° (2θ) range. RigakuD/MAX 2550 diffract meter (CuK radiation, λ = 1.5406 Å) was used, operated at 40 kV and 100 mA. The morphologies were characterized using a scanning electron microscope (SEM, S-4800), transmission electron microscope (TEM, JEM-1400) and High-Resolution Transmission Electron Microscope (HRTEM JEOL JEM-2100F). Element distribution was analyzed by EDS scanning (FESEM, GEmini SEM 500). SERS measurements were performed on a Raman microscope (Renishaw in Via-Reflex), equipped with a 50× objective. 25mW 532 nm laser was used as light source for all SERS measurements unless otherwise stated. The total accumulation time for each SERS spectrum was 20 second. Ultraviolet-visible absorption spectroscopy (UV–vis) was obtained from a UV–vis spectrophotometer (Varian, Cary 500) which was equipped with an integrating sphere assembly. X-ray photoelectron spectroscopy (XPS) was performed using Al Ka radiation with the ESCALAB 250Xi instrument. Electron spin resonance (EPR) was carried out using a Bruker, Karlsruhe (EMX-8/2.7) instrument. The photoluminescence spectra, abbreviated as PL, were obtained using a Hitachi F-4600 fluorescence spectrophotometer at room temperature, wherein the excited wavelength measured 380 nm. The electrochemical impedance spectroscopy (EIS), as well as the photocurrent densities and open-circuit potentials, were evaluated on an electrochemical workstation from Zahner, namely Zennium (The Pt electrode is used as the working electrode, the saturated calomel electrode as the reference electrode, and the ethanol-dispersed catalyst is smeared on the FTO glass as the working electrode). Time-resolved photoluminescence spectroscopy (TRPL) was conducted using a FLSP980 fluorescence lifetime spectrophotometer, with a hydrogen flash lamp of 395 nm wavelength used for excitation.

DRIFTS Spectrum Measurements

The diffuse reflectance infrared Fourier transform spectroscopy (DRIFTS) spectra for H_2O adsorption were acquired using an FTIR spectrometer equipped with a PerkinElmer

spectrum 100 detector, and spectra were obtained from an average of 16 scans with a resolution of 8 cm^{-1}. The catalyst powder was placed in the DRIFTS cell. The atmosphere was first purged with N_2, followed by the introduction of vapors from an aqueous solution containing 10 vol% lactic acid (LA) to establish an environment simulating the reaction conditions. The sample was then irradiated with a 300 W Xe lamp. Spectra were collected at 5-minute intervals for 45 minutes to track the dynamic changes of surface-adsorbed species and reaction intermediates.

DFT Calculation method

We have employed the first principles to perform all Spin-polarization density functional theory (DFT) calculations. The projector augmented wave (PAW) method was employed to describe the interactions between ions and electrons, while the exchange-correlation interactions were treated within the generalized gradient approximation (GGA) using the Perdew-Burke-Ernzerhof (PBE) functional Interlayer van der Waals interactions were corrected using Grimme's DFT-D3 method. A plane-wave energy cutoff of 450 eV was applied. During structural optimization, the convergence thresholds were set at 1×10-5 eV for total energy and below 0.05 eV/Å for Hellmann-Feynman forces. To eliminate periodic image interactions, a vacuum layer thickness of 15 Å was set in the vertical direction. Throughout this work, Brillouin zone sampling was conducted using Monkhorst-Pack grids, with k-point meshes of 2×2×1 for structural optimization and 4×4×1 for density of states calculations.

Photocatalytic activity measurement

The photocatalytic H_2 evolution was measured through the on-line analysis system LabSolar-6A (Perfect Light). Initially, 20 mg of catalyst was dispersed into 90 mL of water, along with 10 mL of DL-Lactic acid (LA) was added as a sacrificial agent. Subsequently, the reaction system was evacuated, and the pressure was approximately 1.0 Kpa. Ar was employed as the carrier gas for H_2 evolution throughout the entire process. The light source was a 300 W Xe lamp with AM 1.5 filter (300 W PLS-SXE300/UV at 10 cm distance), and H_2 were analyzed and identified by gas chromatography (GC SP-7890 Plus). The liquid products were quantified by high performance liquid chromatography (HPLC, SHIMADZU- LC-2050C) equipped with a ShimNex CS C18 (4.6×250 mm) column for

separation. 100 % 1 mM KH_2PO_4 solution was served as the mobile phase with a flow rate of 1.0 mL min^{-1}.

The LA conversion (%) in the photoreforming reaction was calculated according to the following equation:

$$Conversion\ (\%) = \frac{C_0 - C_r}{C_0} \times 100\ \%$$

C_0 denotes the initial concentration of LA reactants, and the concentration of LA reactants after a certain period of the photoreforming reaction is denoted by C_r.

Photoreforming of commercial PLA plastics with H_2 evolution

For the photoreforming of PLA plastics, the PLA hydrolysate obtained via a straightforward hydrothermal process was employed directly. Specifically, 8 g of PLA plastic was added to 80 ml of water, and the mixture was transferred to a 100 mL Teflon-lined stainless-steel autoclave and held at 150 °C for 10 hours. After cooling to room temperature, the resulting PLA hydrolysate was used in the photoreforming reaction. All other conditions were identical to those used in the photoreforming of lactic acid (LA).

The apparent quantum efficiency (AQY)

The apparent quantum efficiency (AQY) of the reaction system was measured using a Xe lamp with light band-pass filter, the Newport 1918-C Optical Meter was used to measure the intensity of incident monochromatic illumination. The AQY is calculated by using the following equation.

$$AQY = \frac{2MN_Ahc}{It\lambda} \times 100\%$$

Where M is molar amounts of H_2 during irradiation 2 h, N_A is Avogadro constant (6.022 ×1023 mol^{-1}). h is Planck constant (6.626×10^{-34} J·s). c is the light velocity (3×10^8 m/s). I is the intensity of irradiation light (mW). t is the reaction time (7200 s). λ is the wavelength of the monochromatic light(m).

2. Supplementary figures

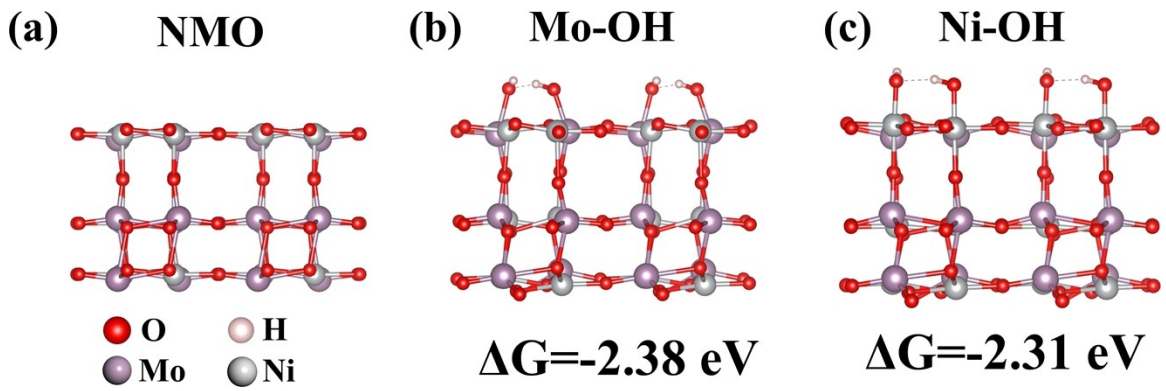

Figure S1. Lattice structure of (a) NMO. Gibbs free energy after introduction of hydroxyl groups at Mo sites (b) and Ni sites (c).

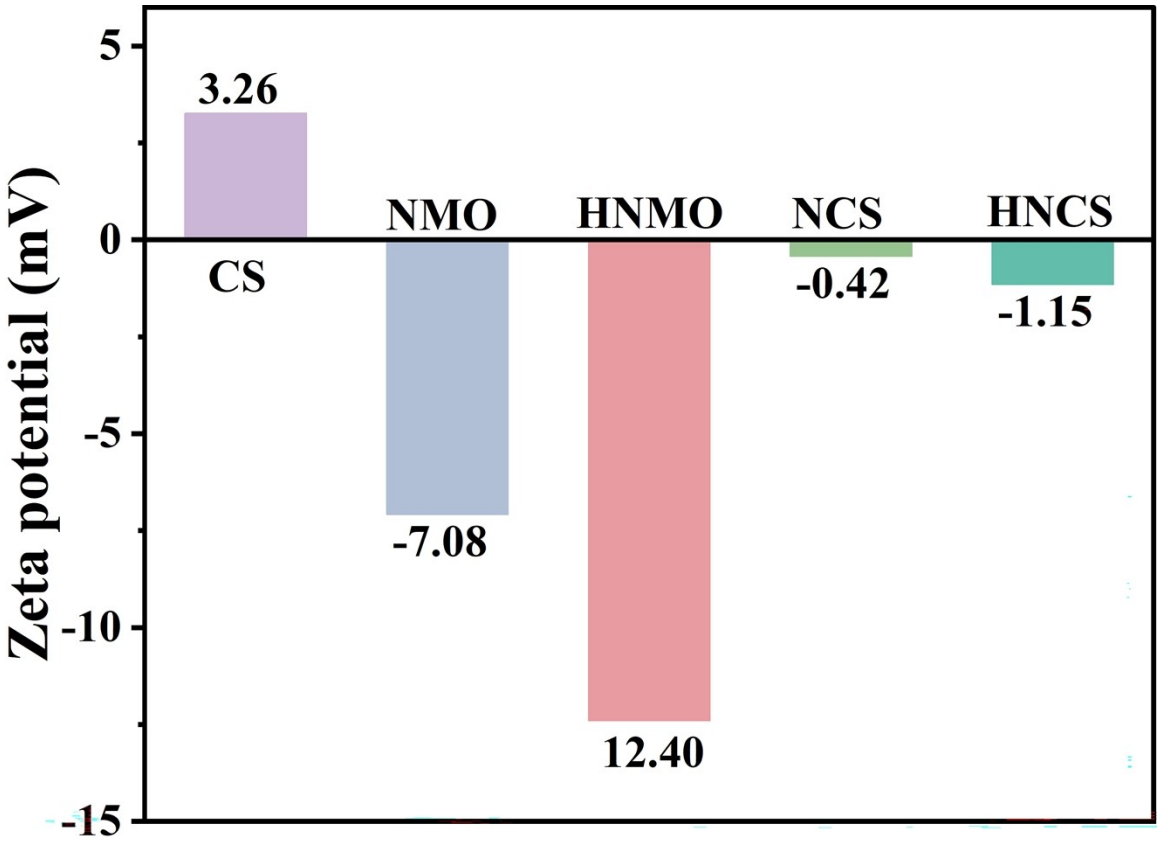

Figure S2. Zeta potential plots for each sample.

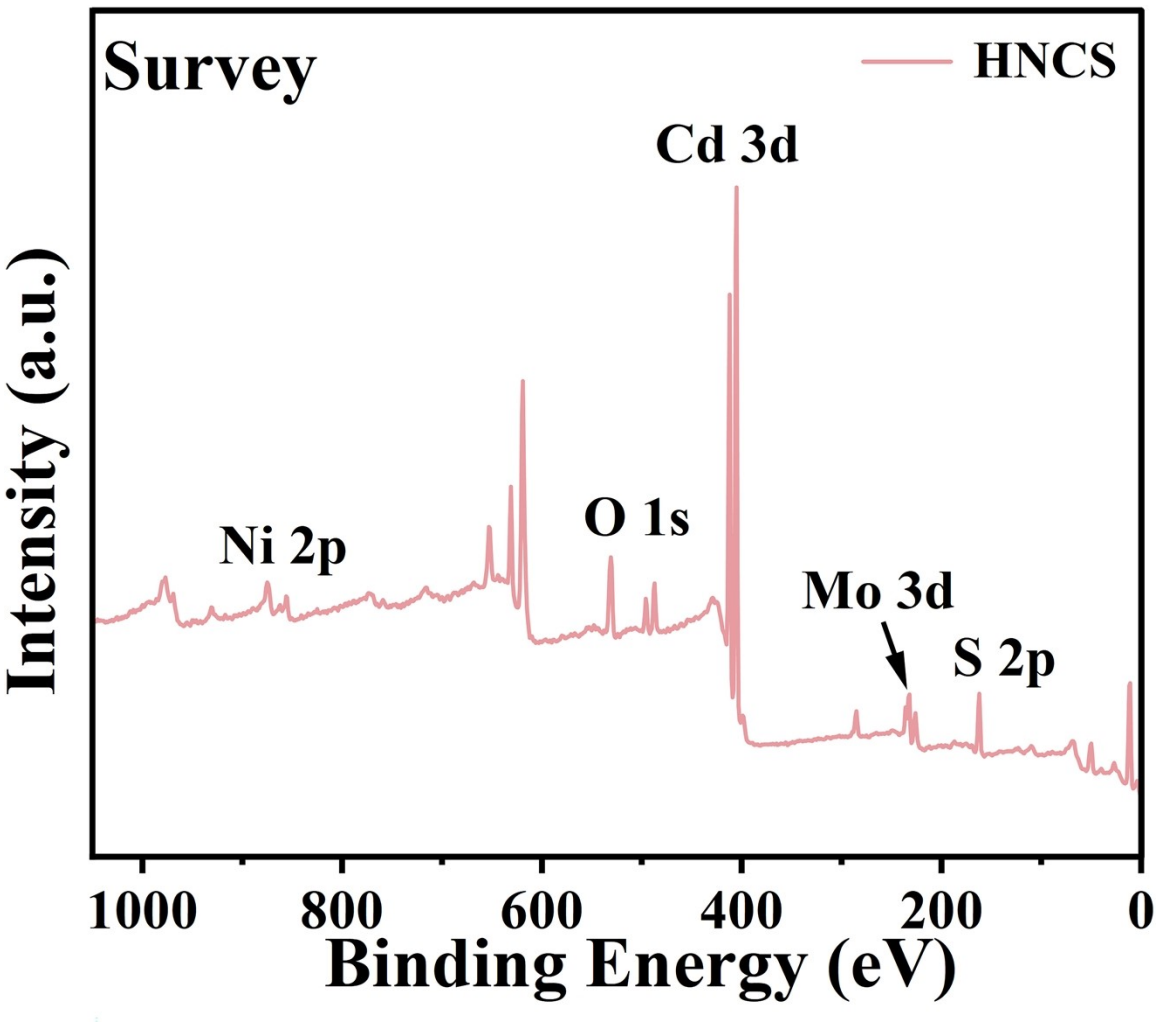

Figure S3. The survey XPS spectrum of HNCS.

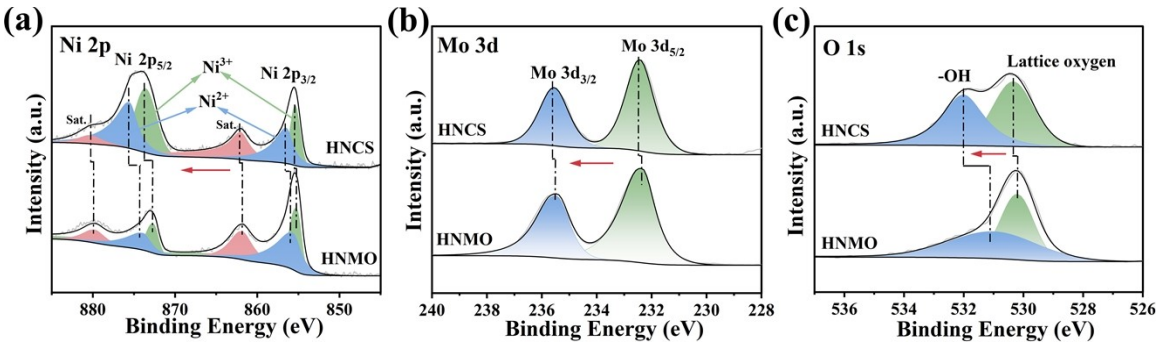

Figure S4. High resolution XPS spectra of a) Ni 2p, b) Mo 3d, c) O 1s of HNCS and HNMO.

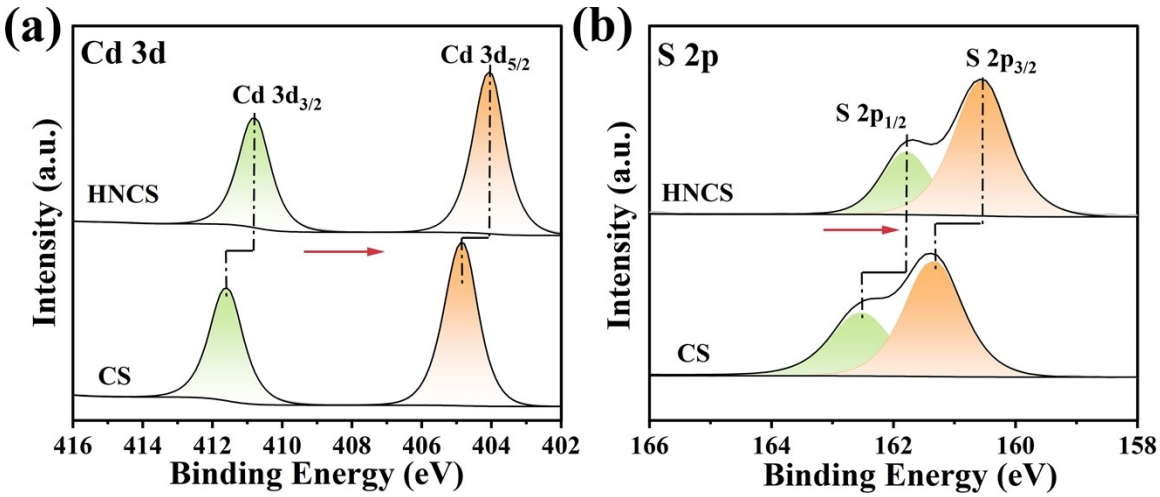

Figure S5. High resolution XPS spectra of a) Cd 3d, b) S 2p of HNCS and CS.

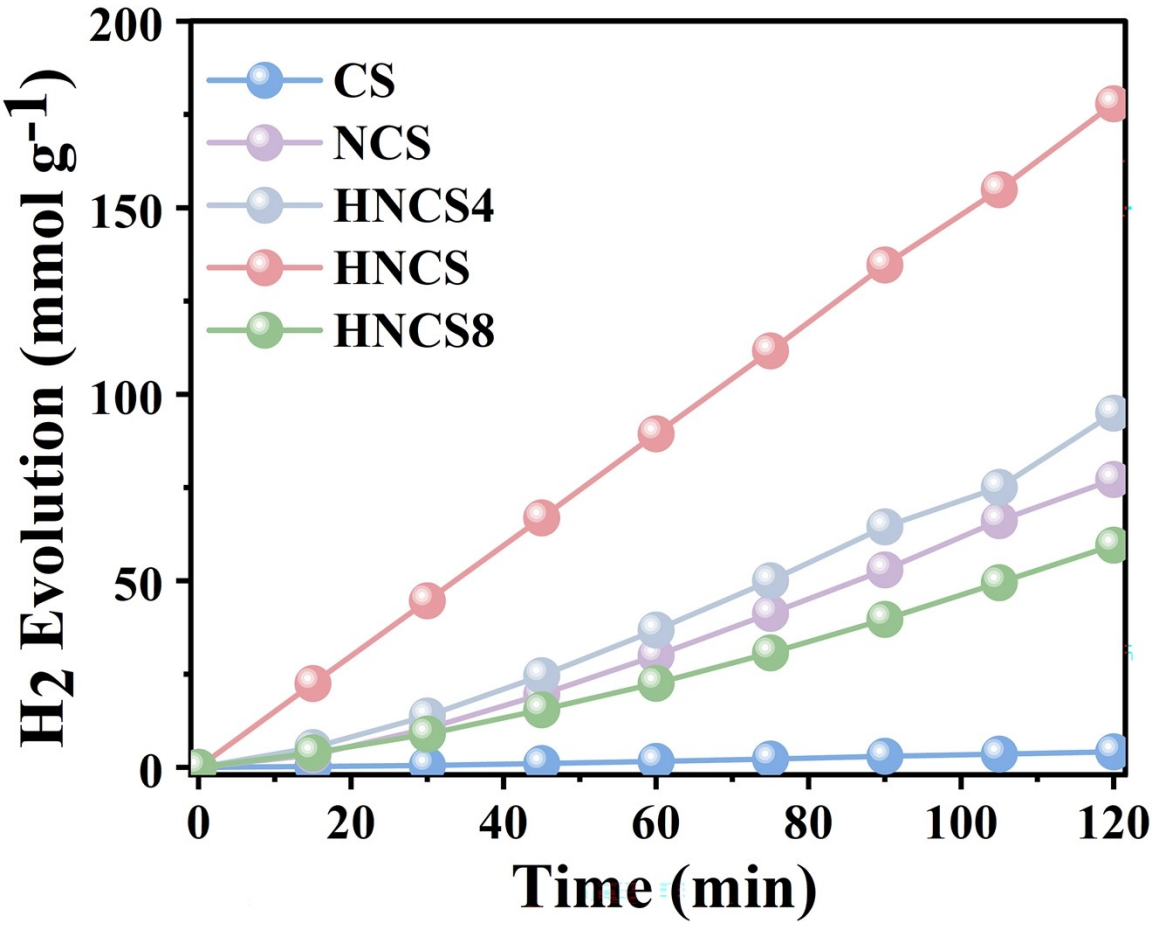

Figure S6. Photocatalytic H_2 production of the synthesized samples.

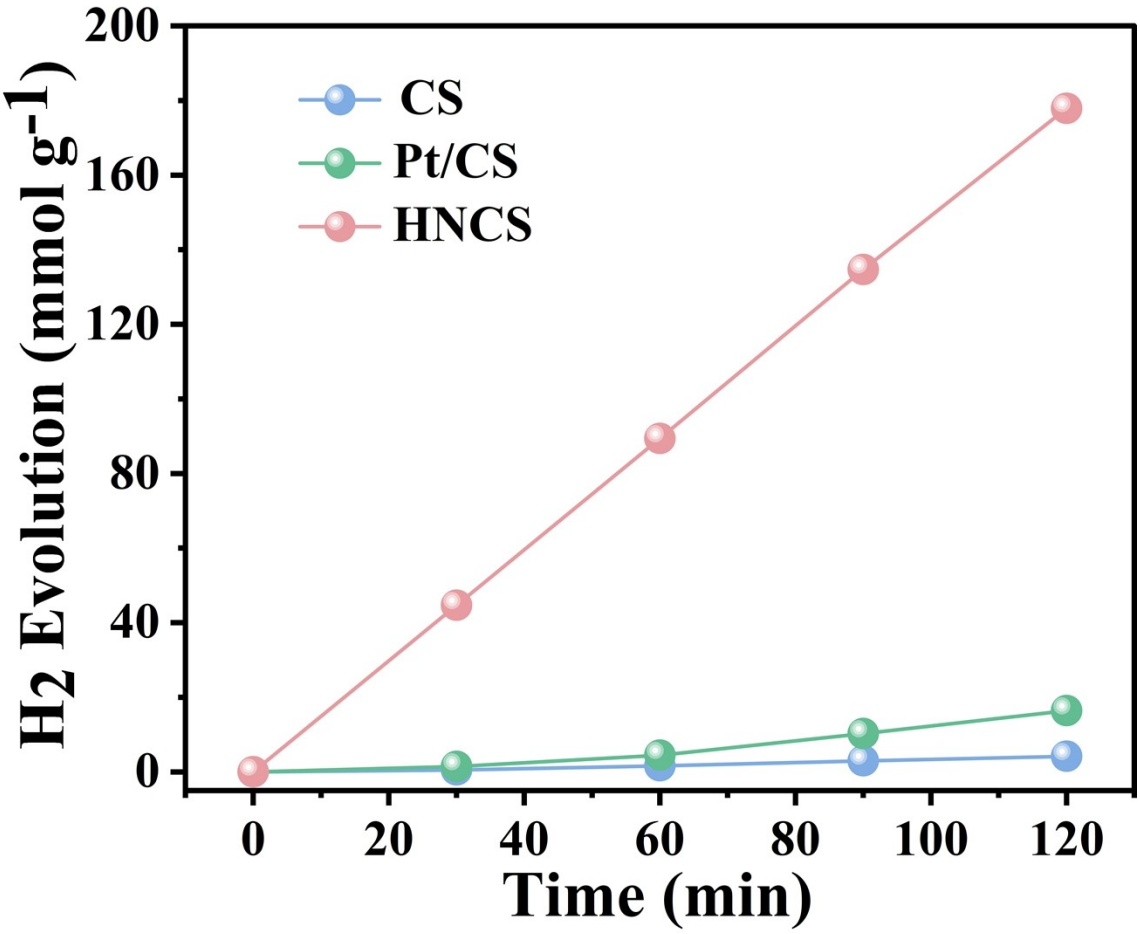

Figure S7. Photocatalytic H_2 production of the synthesized samples.

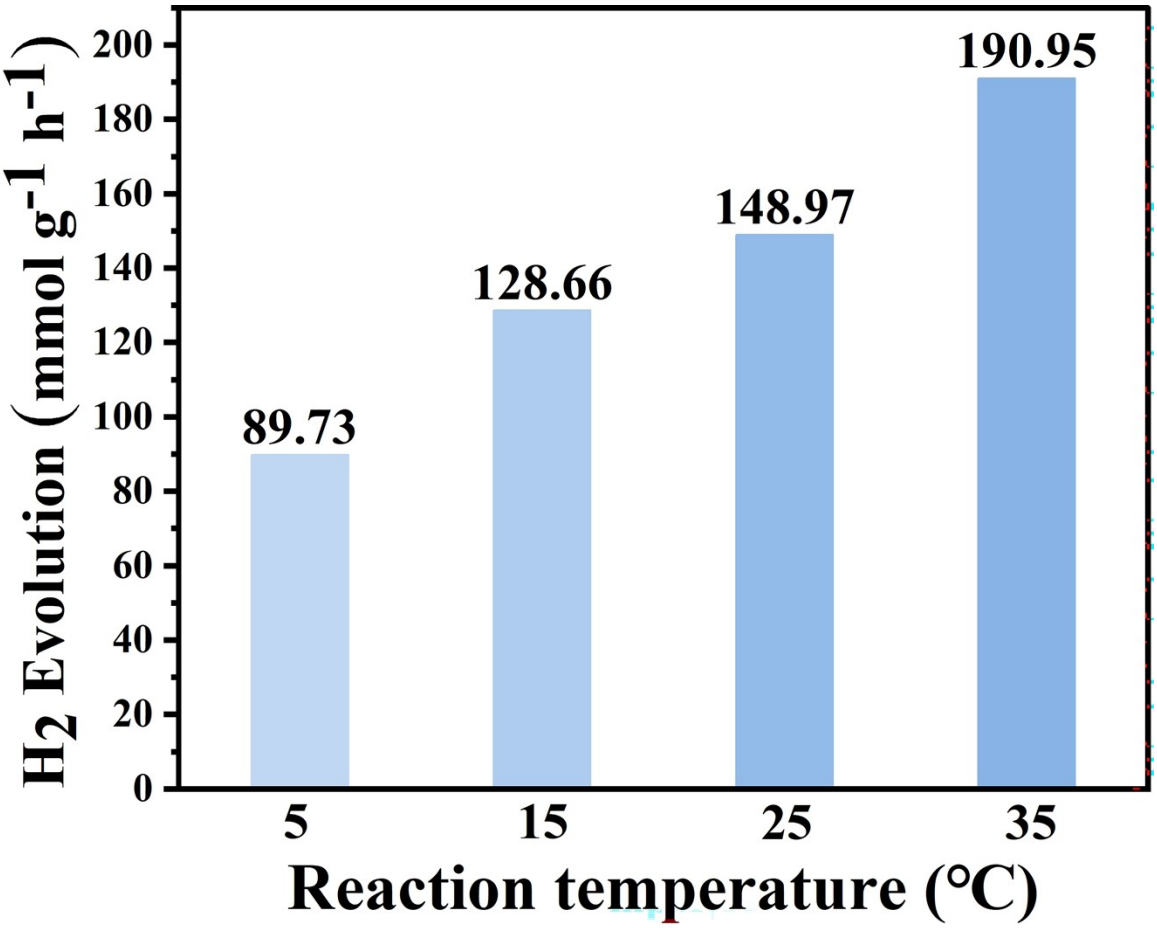

Figure S8. The photocatalytic H_2 evolution activities of HNCS under different reaction temperature.

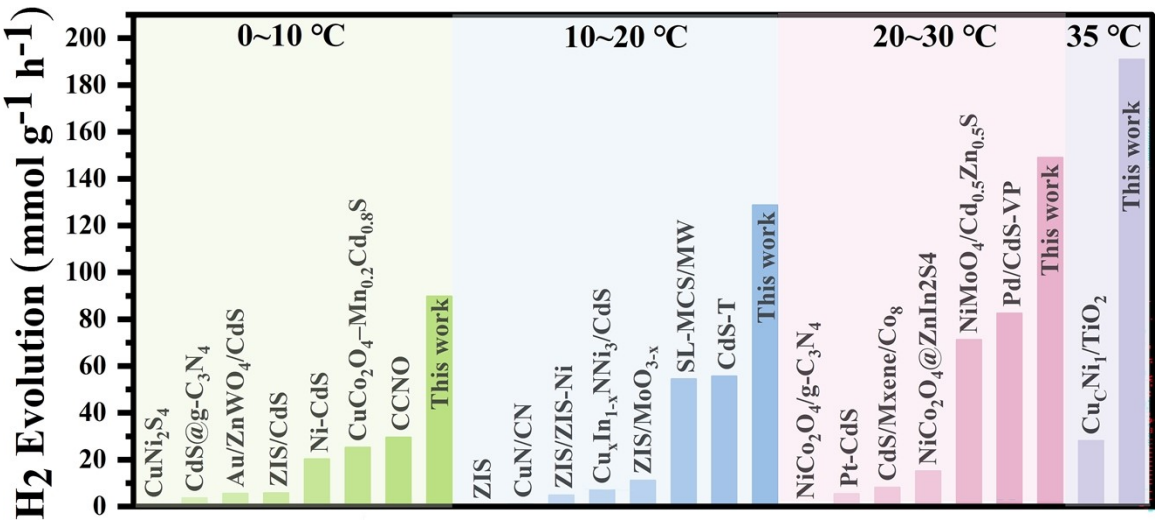

Figure S9. The photocatalytic H_2 evolution performance of HNCS in this work compared with reported photocatalysts.

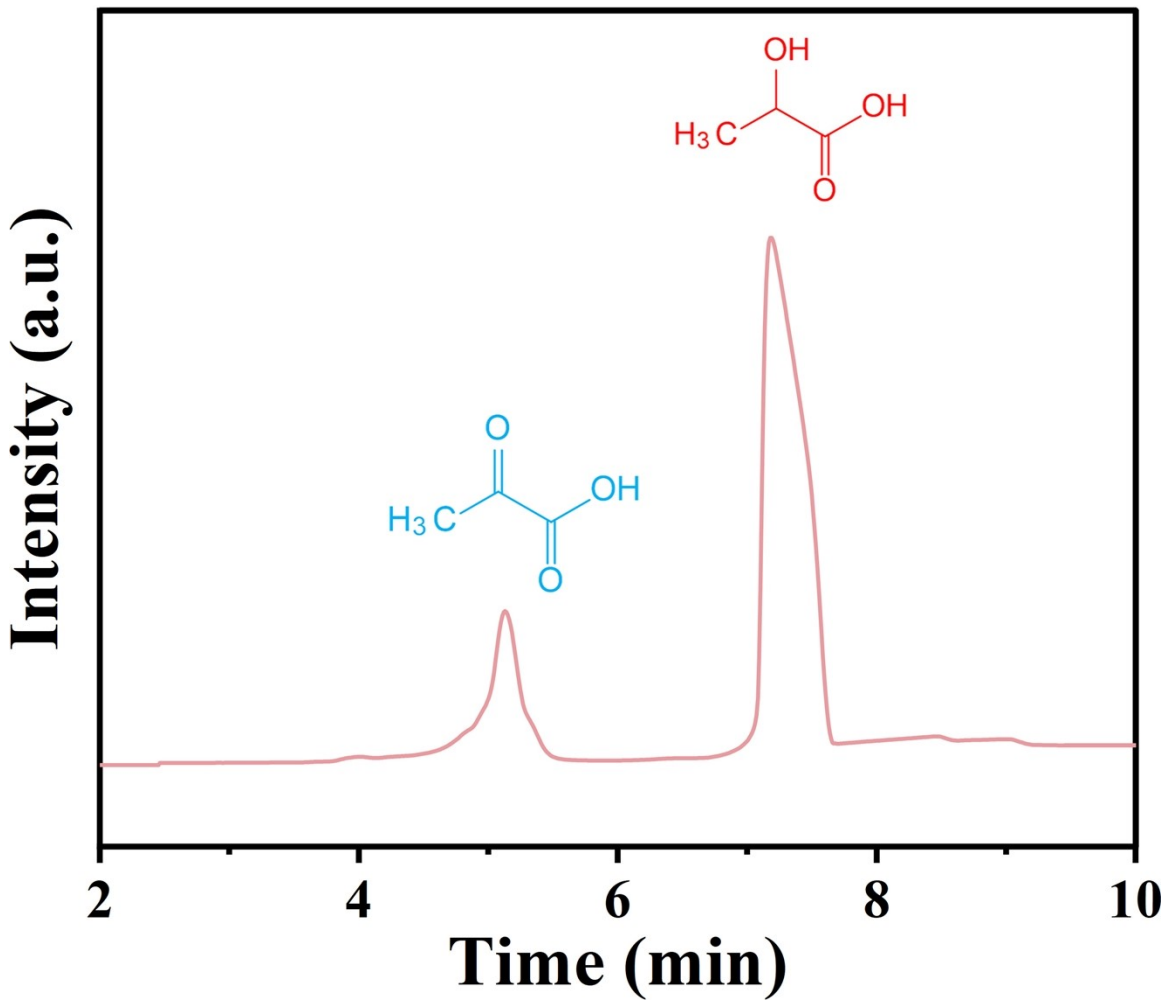

Figure S10. HPLC result of the photoreforming LA aqueous solution after 2-hour reaction over HNCS.

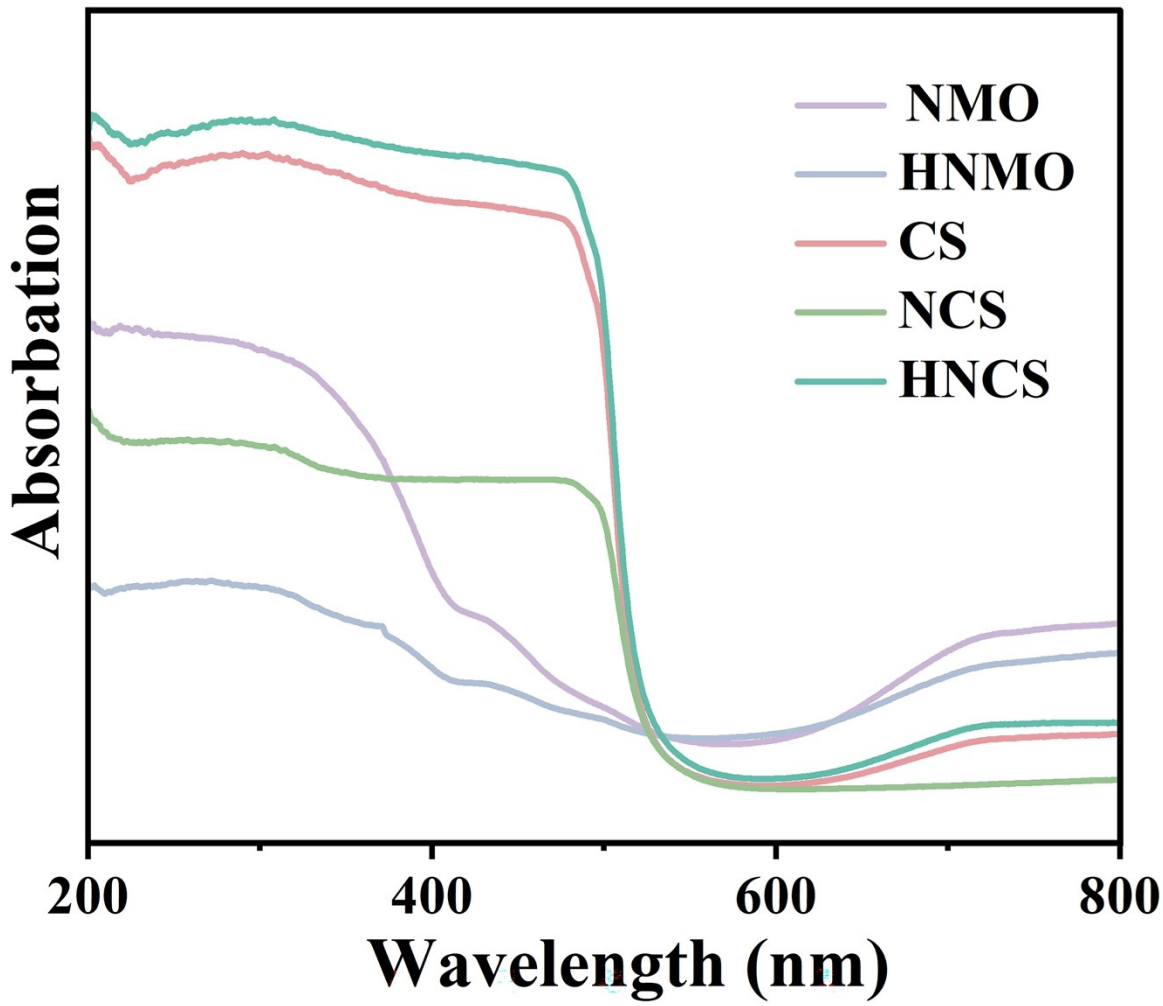

Figure S11. UV-vis DRS of CS, NMO, HNMO, NCS and HNCS.

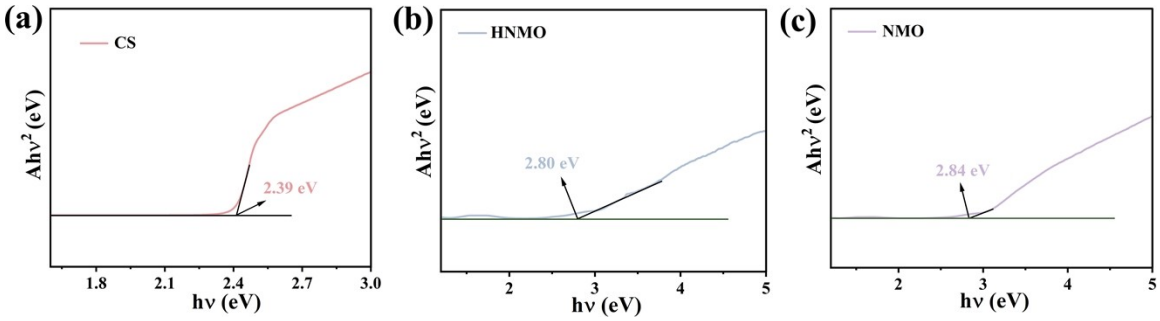

Figure S12. Band gap energy of a) CS, b) HNMO and c) NMO.

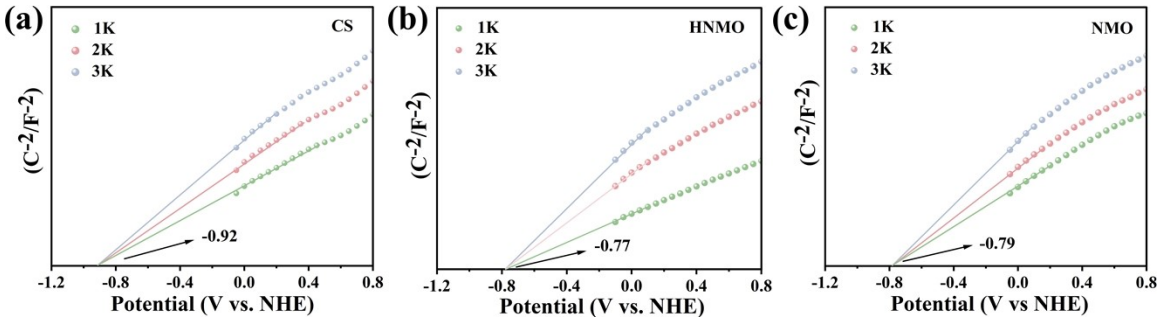

Figure S13. Mott-schottky diagram of a) CS, b) HNMO and c) NMO.

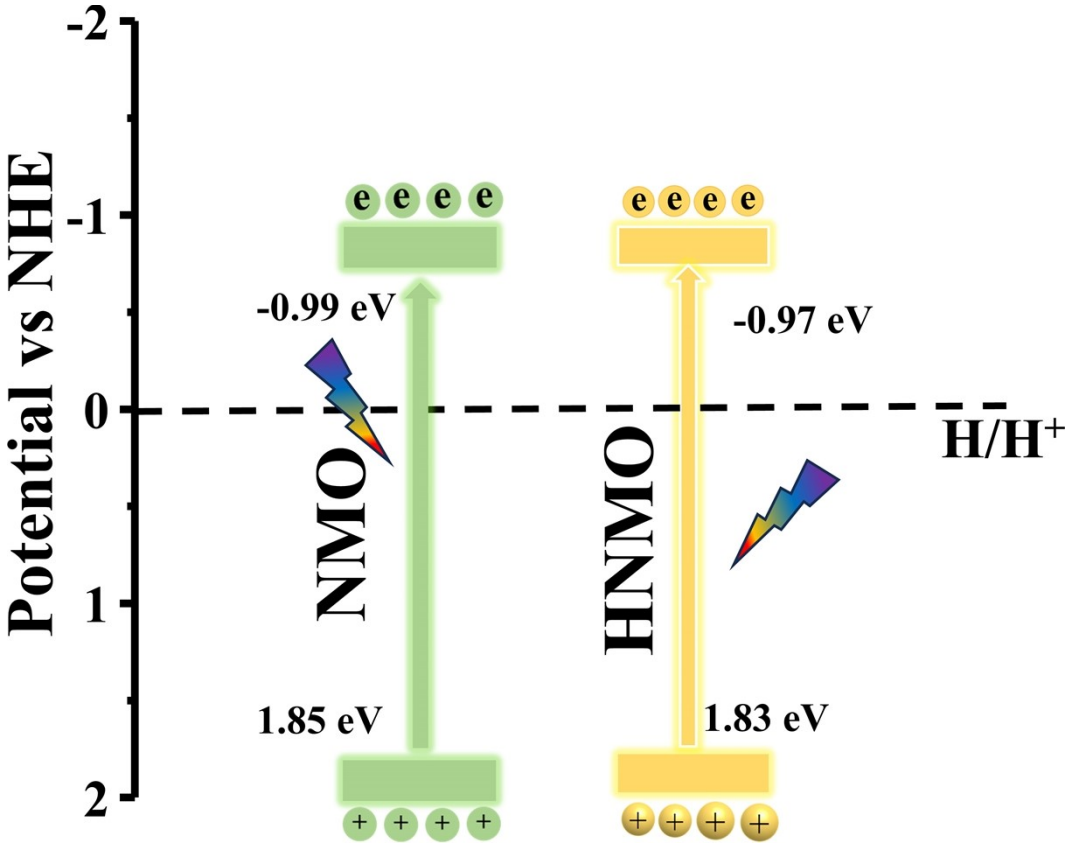

Figure S14. Schematic diagram of the band structure of HNMO and NMO.

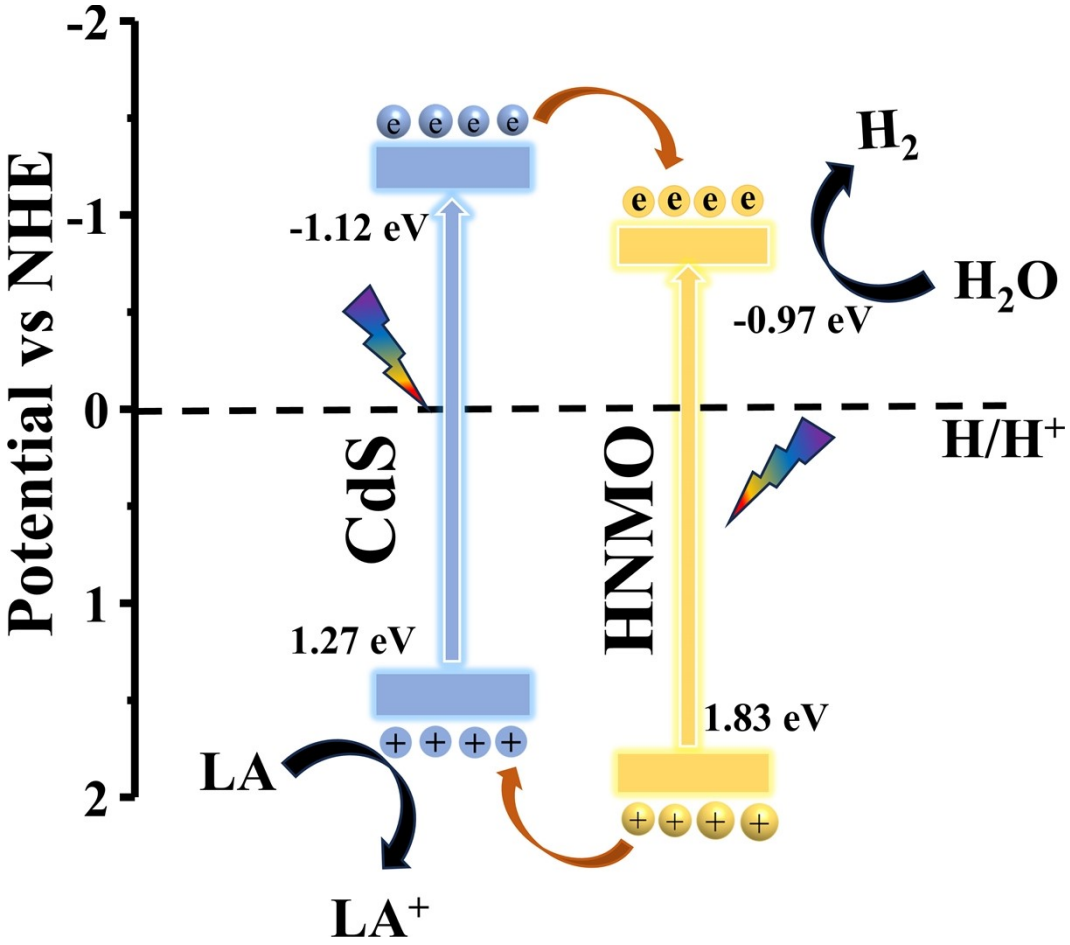

Figure S15. Schematic diagram of the band structure.

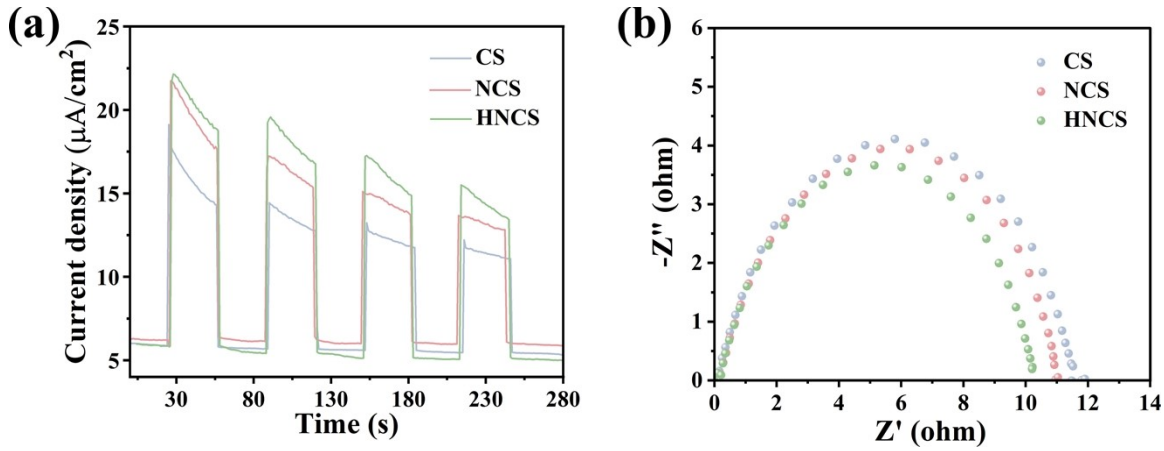

Figure S16. a) The TPR spectra and b) EIS Nyquist plots of CS, NCS and HNCS under visible light irradiation in Na_2SO_4 solution.

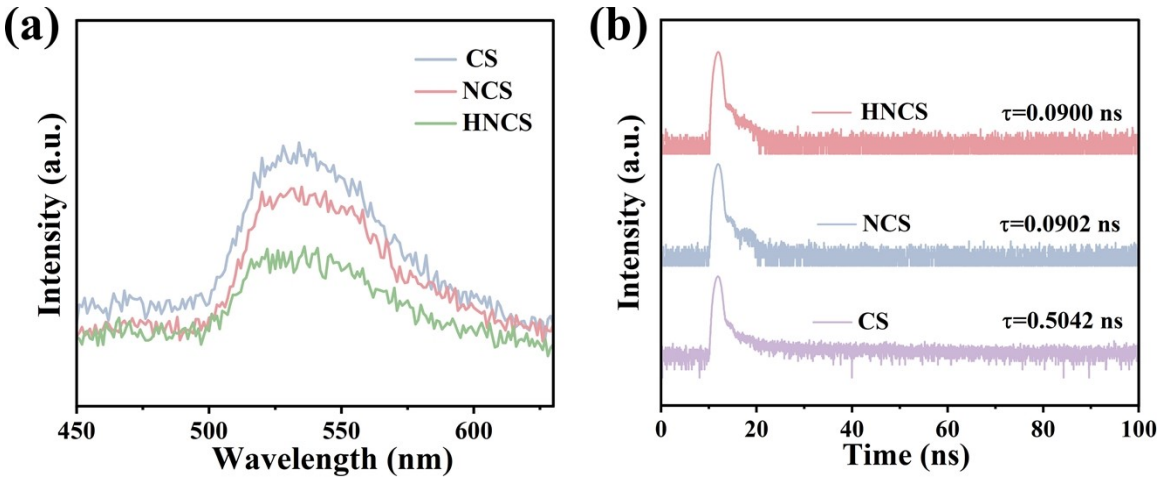

Figure S17. a) The PL spectra of CS, NCS and HNCS. b) The TRPL spectra of CS, NCS and HNCS.

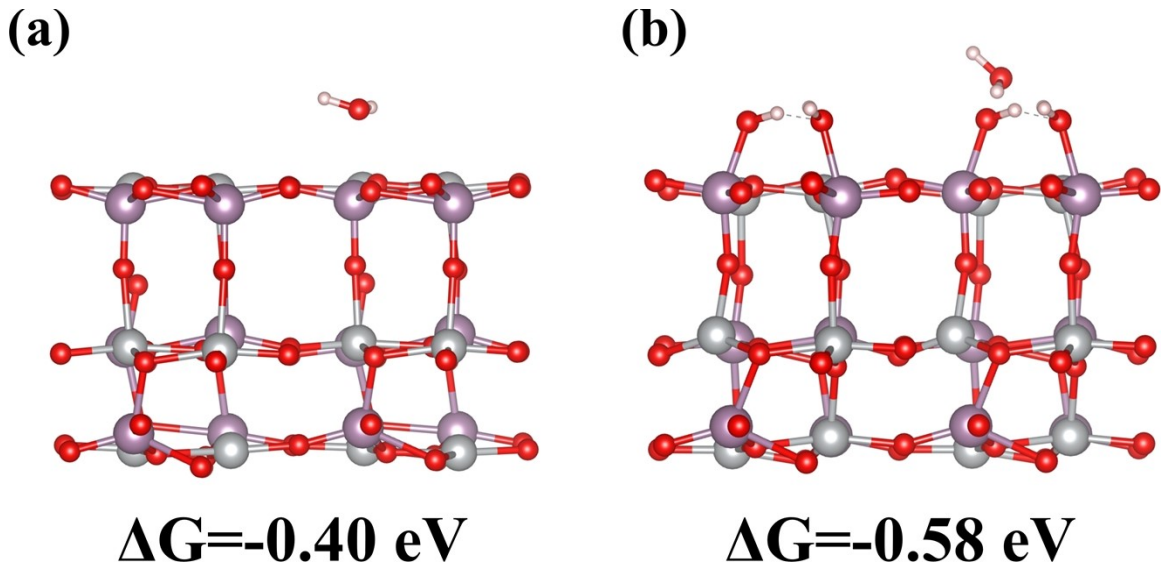

Figure S18. Calculated adsorption configurations and energies of a water molecule on the a) NMO and b) HNMO surfaces.

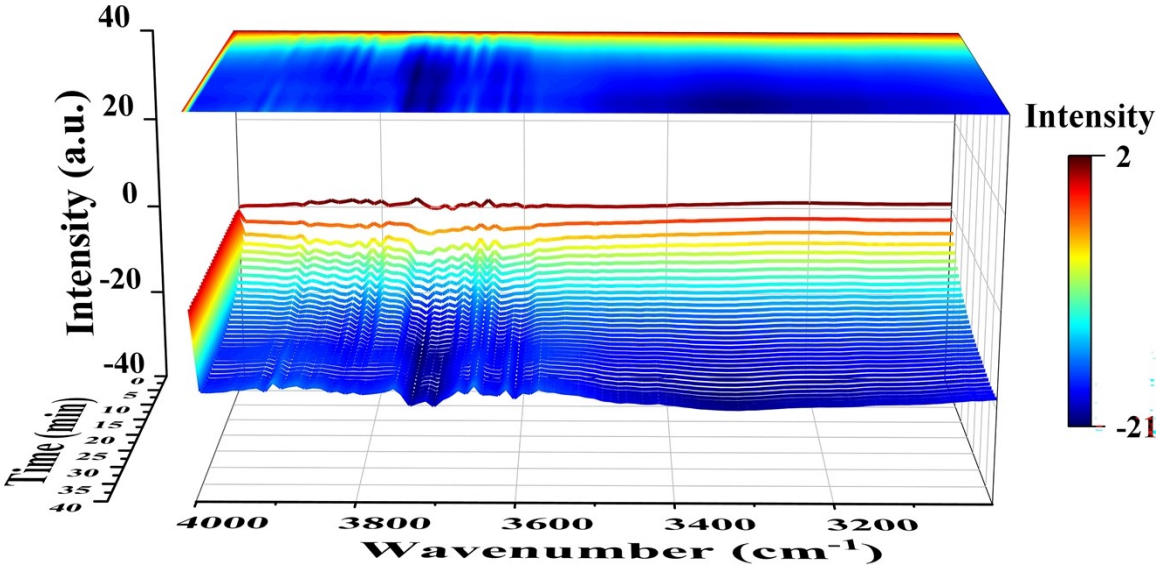

Figure S19.The DRIFTS spectra of NCS.

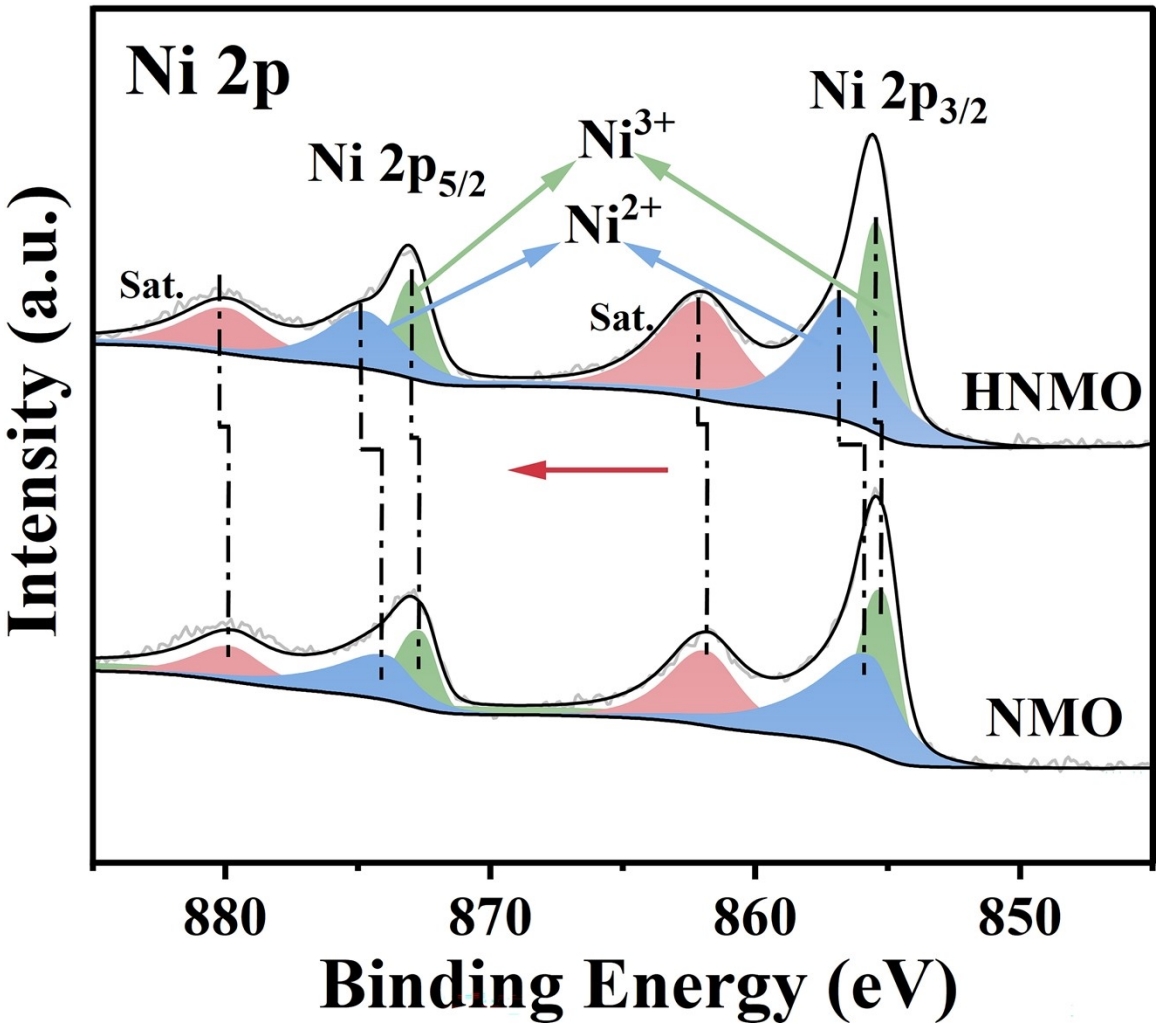

Figure S20. High resolution XPS spectra of Ni 2p of NMO and HNMO.

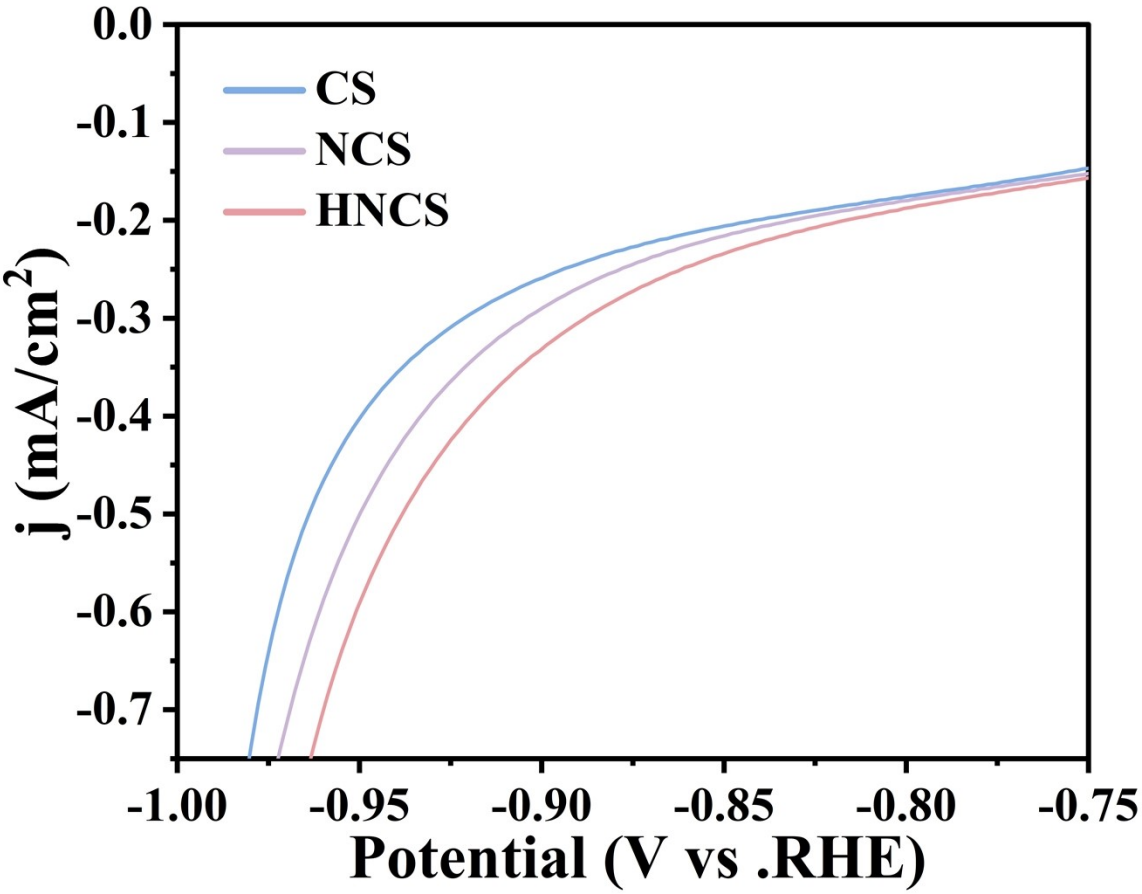

Figure S21. Linear sweep voltammetry (LSV) polarization curves of CS, NCS and HNCS in a 0.5 M Na_2SO_4 solution.

3. Supplementary tables

Table S1. The summary of elemental composition of HNCS through EDS analysis.

Element	At%
Cd	30.03
S	36.09
Ni	4.64
Mo	3.75
O	25.48

Table S2. The summary of elemental composition of HNCS through XPS analysis.

Element	At%
Cd	31.63
S	34.60
Ni	5.52
Mo	4.48
O	23.77

Table S3. Wavelength-depended AQY of HNCS.

Wavelength (nm)	Intensity of incident light (mW)	Molar amounts of H_2 (μmol)	AQY (%)
365	80.1	176.4	19.7
420	72.6	501.6	53.8
475	78.0	781.9	69.0
520	66.6	60.9	5.7

Table S4. Comparison of hydrogen precipitation performance of the same type of photocatalysts.

Photocatalyst	H_2 evolution (mmol g^{-1} h^{-1})	AQY (%)	Ref
$NiCo_2O_4$/g-C_3N_4	0.462	-	[1]
Mo/S-BiOBr	0.711	13.9	[2]
$CuNi_2S_4$	1	-	[3]
ZnNiOS	3.375	28.5	[4]
NZM/CdS	5.335	9.3	[5]
Au/$ZnWO_4$/CdS	5.484	2.62	[6]
Ni/NiOx@C/g-C_3N_4	10.7	40.78	[7]
$NiCo_2O_4$@$ZnIn_2S_4$	15.11	-	[8]
$K_3PW_{12}O_40$/CdS	18.7	-	[9]
FeS_2/$CuCo_2O_4$	19.5	19.8	[10]
$CuCo_2O_4$–$Mn_{0.2}Cd_{0.8}S$	25.17	-	[11]
CCNO	29.51	66.86	[12]
WO_3/CdS	34.119	-	[13]
$NiMoO_4$/$Cd_{0.5}Zn_{0.5}S$	71.2	8.23	[14]
This work	89.37	-	-

Table S5. The photocatalytic H_2 evolution performance of HNCS in this work compared with reported photocatalysts under different reaction temperature.

Photocatalyst	H_2 evolution (mmol g^{-1} h^{-1})	Reaction temperature (℃)	Ref
$CuNi_2S_4$	1	0	[3]
CdS@g-C_3N_4	3.54	5	[15]
Au/$ZnWO_4$/CdS	5.484	4	[6]
ZIS/CdS	5.678	6	[16]
Ni-CdS	20.28	5	[17]
$CuCo_2O_4$–$Mn_{0.2}Cd_{0.8}S$	25.17	6	[11]
CCNO	29.51	6	[12]
This work	89.73	5	-
ZIS	0.227	10	[18]
CuN/CN	1.074	10	[19]
ZIS/ZIS-Ni	4.83	10	[20]
$Cu_xIn_{1-x}NNi_3$/CdS	6.945	20	[21]
ZIS/MoO_{3-x}	11.08	10	[22]
SL-MCS/MW	54.4	10	[23]
CdS-T	55.61	20	[24]
This work	128.66	15	-
$NiCo_2O_4$/g-C_3N_4	0.462	25	[1]
Pt-CdS	5.4	25	[25]
CdS/Mxene/Co_8	8.13	25	[26]
$NiCo_2O_4$@$ZnIn_2S_4$	15.11	25	[8]
$NiMoO_4$/$Cd_{0.5}Zn_{0.5}S$	71.2	30	[14]
Pd/CdS-VP	82.5	25	[27]
This work	148.97	25	-
Cu_CNi_1/TiO_2	28.03	35	[28]
This work	190.95	35	-

Table S6. Summary of the photoluminescence decay time (τ) and the relative intensities of CS, NCS, HNCS.

Samples	τ_1**(ns)**	τ_2**(ns)**	A_1	A_2	**Average lifetime (τ,ns)**
CS	0.1371	14.5918	97.46	2.54	0.5042
NCS	0.0401	14.7950	99.66	0.34	0.0902
HNCS	0.0357	18.1392	99.70	0.30	0.0900

The average lifetime was calculated using the equation: $\tau = (\tau_1^2 A_1 + \tau_2^2 A_2)/(\tau_1 A_1 + \tau_2 A_2)$

4. References

1. J. Liu, J. Zhang, D. Wang, D. Li, J. Ke, S. Wang, S. Liu, H. Xiao and R. Wang, *ACS Sustainable Chem. Eng.*, 2019, **7**, 12428-12438.
2. Z. Su, B. Wu, D.-H. Kuo, L. Chen, P. Zhang, B. Yang, X. Wu, D. Lu, J. Lin and X. Chen, *J. Mater. Chem. A*, 2024, **12**, 28486-28502.
3. B. Zhao, M. Shakouri, R. Feng, T. Regier, Y. Zeng, Y. Zhang, J. Zhang, L. Wang, J. L. Luo and X. Z. Fu, *Small Methods*, 2023, **7**, 2201612.
4. N. S. Gultom, H. Abdullah and D.-H. Kuo, *Appl. Catal., B*, 2020, **272**, 118985.
5. J. Liu, X. Yang, X. Guo and Z. Jin, *J. Mater. Sci. Technol.*, 2024, **196**, 112-124.
6. W. Wu, N. Zhang and Y. Wang, *Adv. Funct. Mater.*, 2024, **34**, 2316604.
7. Z. Yang, T. Huang, M. Li, X. Wang, X. Zhou, S. Yang, Q. Gao, X. Cai, Y. Liu and Y. Fang, *Adv. Mater.*, 2024, **36**, 2313513.
8. W. Li, G. Zuo, S. Ma, L. Xi, C. Ouyang, M. He, Y. Wang, Q. Ji, S. Yang and W. Zhu, *Appl. Catal., B*, 2025, **365**, 124971.
9. L. Sun, X. Yu, L. Tang, W. Wang and Q. Liu, *Chin. J. Catal.*, 2023, **52**, 164-175.
10. Z. He, K. Lin, N. H. Wong, J. Sunarso, Y. Xia, X. Fu, B. Tang, Z. Huang, Y. Wang and H. Yang, *Nano Energy*, 2024, **124**, 109483.
11. J. Peng, T. Han, Q. Liu, W. Luan, R. Zhao, J. Han and L. Wang, *Mater. Today Chem.*, 2024, **36**, 101973.
12. Y. Zhang, N. Cao, X. Liu, F. He, Y. Lu, S. Wang, C. Zhao, Y. Wang, J. Zhang and S. Wang, *ACS Catal.*, 2024, **14**, 13768-13780.
13. Z. Liu, F. Jin, X. Li, P. Zhang and Z. Jin, *J. Mater. Sci. Technol.*, 2024, **188**, 131-143.
14. J. Tian, X. Cao, T. Sun, H. Miao, Z. Chen, W. Xue, J. Fan and E. Liu, *Composites, Part B*, 2024, **277**, 111389.
15. Y. Zhang, X. Ran, H. Fu, Y. Gong, S. Li, F. Gu, S. Wang, X. An, D. Su and X. Yang, *Adv. Funct. Mater.*, 2024, **34**, 2404585.
16. D. Zhang, Z. Gao, D. Yang, L. Wang, X. Yang, K. Tang, H. Yang, X. Zhan, Z. Wang and W. Yang, *Carbon Energy*, 2025, e707.
17. F. Wu, X. Zhang, L. Wang, G. Li, J. Huang, A. Song, A. Meng and Z. Li, *Small*, 2024, **20**, 2309439.

18. N. Xi, E. C. dos Santos, X. Zhao, C. Cui, M. Lill, H. Lundberg, Y. Sang, H. Liu and X. Yu, *Nano Energy*, 2025, **136**, 110750.
19. G. Wu, X. Gao, P. Sun, Z. Mo, Q. Wang, H. Chen, H. Liao, P. Yan, X. She and H. Xu, *Appl. Catal., B*, 2025, **371**, 125265.
20. W. Wang, J. Liu, M. Cui, X. Li, L. Niu, X. Wu, Y. Chen, X. Li, H. Zhu and D. Wang, *Chem. Eng. J.*, 2025, **507**, 160370.
21. H. Huang, Z. Chen, Y. Yang, Y. Lin, Y. Fan, X. Wu, Y. Ji, Y. Wang, C. Yang and Y. Yu, *Adv. Funct. Mater.*, 2025, **35**, 2414298.
22. R. Liu, Y. Cui, T. Wang, J. Liu, B. Liu, S. Zuo and H. Yu, *J. Mater. Chem. A*, 2025, **13**, 8144-8156.
23. S. Wan, W. Wang, B. Cheng, G. Luo, Q. Shen, J. Yu, J. Zhang, S. Cao and L. Zhang, *Nat. Commun.*, 2024, **15**, 9612.
24. M. Dan, S. Yu, W. Lin, M. Abdellah, Z. Guo, Z. Q. Liu, T. Pullerits, K. Zheng and Y. Zhou, *Adv. Mater.*, 2025, **37**, 2415138.
25. H. Liu, J. Peng, X. Zhang, K. Zheng, L. Zheng, K. Lv, Q. Li and P. Zhou, *Chem. Eng. J.*, 2025, **504**, 158618.
26. Y. Feng, X. Fang, J. Zang, B. Song, C. Hu, X. Dong and Y. Ding, *Sci. China:Chem.*, 2025, **68**, 772-780.
27. H. Li, R. Li, Y. Jing, B. Liu, Q. Xu and T. Tan, 2024.
28. Y. Feng, S. Gong, Y. Wang, C. Ban, X. Qu, J. Ma, Y. Duan, C. Lin, D. Yu and L. Xia, *Adv. Mater.*, 2025, **37**, 2412965.